Inorganic Chemistry
Communication
pubs.acs.org/IC

"Criss-Crossed" Dinucleating Behavior of an N4 Schiff Base Ligand: Formation of a μ-OH,μ-O_2 Dicobalt(III) Core via O_2 Activation

Yae In Cho, David M. Joseph, and Michael J. Rose*

Department of Chemistry, The University of Texas at Austin, Austin, Texas 78713, United States

Supporting Information

ABSTRACT: We report the synthesis and structural characterization of a dicobalt(III) complex with a μ-OH,μ-O_2 core, namely μ-OH,μ-O_2-$[Co(enN4)]_2(X)_3$ [$\mathbf{1(ClO_4)_3}$ and $\mathbf{1(BF_4)_3}$]. The dinuclear core is cross-linked by two N4 Schiff base ligands that span each cobalt center. The formally $Co^{III}-Co^{III}$ dimer is formed spontaneously upon exposure of the mononuclear Co(II) complex to air and exhibits a ν(O−O) value at 882 cm^{-1} that shifts to 833 cm^{-1} upon substitution with $^{18}O_2$. The CV of $\mathbf{1(BF_4)_3}$ exhibits a reversible $\{Co^{III}-Co^{III}\}\leftrightarrow\{Co^{III}-Co^{IV}\}$ redox process, and we have investigated the oxidized $\{Co^{III}-Co^{IV}\}$ species by EPR spectroscopy (g = 2.02, 2.06; S = 1/2 signal) and DFT calculations.

At the turn of the last century, Alfred Werner described the preparation of coordination complexes containing a dicobalt core with a stabilized dioxygen ligand, and the remaining coordination sphere was proposed to be occupied by an array of ammine ligands.[1,2] However, the exact structure and designation of the core dioxygen ligand was controversial for some time. Nearly 100 years after Werner's initial report of the crystalline dioxygen-activated dicobalt species, Werner's historical sample was characterized by X-ray crystallography and reported as μ-OH,μ-O_2,μ-NH_2-$[\{Co(NH)_3\}_2](NO_3)_3$.[3]

Such dicobalt, dioxygen adducts are kinetically stable, and have been investigated as O_2 carriers in photochemical studies[4] or as artificial O_2 carriers for biomedical applications. Dicobalt(III) dioxygen adducts have also been studied as small molecule models[5] relevant to heterogeneous oxygen evolving materials, such as cobalt oxide (Co_2O_3).[6] There are two predominant O_2 binding motifs: the singly bridged μ-peroxo species and the doubly bridged μ-hydroxo,μ-peroxo species. Such complexes are supported by mono-, bi-, or tetradentate nitrogenous ligands (NH_3, bpy, en, Me_2teta), as well as mixed N,O donor sets (salen).[7] In each case, the only linkage between the two metal centers is the hydroxo or peroxo bridge (i.e., not the chelate). In this work, we report the formation, structure, and properties of a μ-$(\mathbf{L}_{N4})_2$,μ-hydroxo,μ-peroxo-dicobalt core supported by a dinucleating motif of a simple N4 Schiff base ligand.

Reaction of the Schiff base ligand N,N-bis(pyridin-2-ylmethylene)ethane-1,2-diimine (enN4) with $[Co(H_2O)_6](BF_4)_2$ in aerobic MeCN with excess pyridine (~10 equiv) results in the formation of a dark blackish-orange solution. Vapor diffusion of Et_2O into this solution yielded black blocks suitable for X-ray diffraction.The molecular structure is shown in Figure 1. The structure exhibits a dicobalt system bridged by (i) a μ-OH,μ-O_2 core and (ii) a stretched enN4 ligand frame [N2−C7−C8 = 114.2(3)°; N3−C8−C7 = 117.6(3)°] that spans both cobalt ions. The two enN4 ligands cochelate the cobalt centers in a diagonal fashion that criss-crosses the μ-OH,μ-O_2 dicobalt core. The peroxo bridge is slightly disordered across diagonal orientations (89/11%; see Supporting Information Figure S1). We designate the compound as μ-OH,μ-O_2-$[Co(enN4)]_2(BF_4)_3$, or $\mathbf{1(BF_4)_3}$.

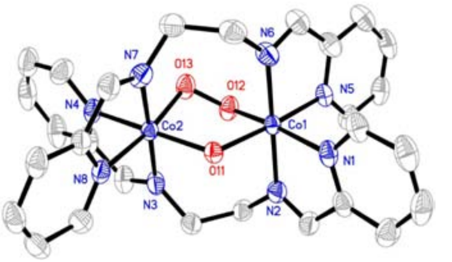

Figure 1. ORTEP diagram (50% ellipsoids) of the cation in μ-OH,μ-O_2-$[Co(enN4)]_2(BF_4)_3$ ($\mathbf{1(BF_4)_3}$). H's are not shown for sake of clarity. Selected bond distances (Å): Co1−N1 = 1.994(3); Co1−N2 = 1.922(3); Co−O12 = 1.858(3); Co−O11 = 1.886(2).

There are a number of similar μ-OH,μ-O_2 dicobalt cores supported by N-containing ligands that have been structurally characterized (see Table S2). For example, the complexes μ-OH,μ-O_2-$[\{Co(en)_2\}_2]$ (en = ethylenediamine) and μ-OH,μ-O_2-$[\{Co(bpy)_2\}_2]$ (bpy =2,2′-bipyridine) exhibit the analogous core structure without the support of the N4-type dinucleating ligand.[4,8] In the tren [tren = tris(2-aminoethyl)amine)] and Me_2teta [Me_2teta = N,N-(dimethyl)triethylenetetramine] derivatives μ-OH,μ-$O_2[(\mathbf{L})_2Co]_2(ClO_4)_3$, the ligands simply cap each cobalt center, with no interconnection of the ligand across the two cobalt centers.

The two Co−O(O) bond lengths of 1.839(3) (Co1−O12) and 1.858(3) Å (Co2−O13) are quite short when compared to other tetraimine ligated μ-OH,μ-O_2 complexes [range =1.860(2) to 1.877(4) Å] of the type μ-OH,μ-$O_2[(bpy)_2Co]_2^{3+}$; similar complexes derived from alkyl amines (en, tren, Me_2teta) are also longer [range = 1.857−1.947 Å].[8] The observed peroxo bond [O−O = 1.401(3) Å] (O12−O13) is shorter than that found in the bpy derivatives [1.415(6), 1.412(3) Å] and most of the alkylamine derivatives [range =

Received: September 23, 2013
Published: November 15, 2013

1.430−1.462 Å]. Two exceptions of note are the en dimer μ-OH,μ-O_2-$[(en)_2Co]_2(NO_3)_3$ [O−O = 1.339 Å] and the Werner complex μ-OH,μ-O_2,μ-NH_2-$[(NH_3)_3Co]_2(NO_3)_3$ [O−O = 1.340(4) Å], which exhibits an anionic amido bridge in addition to the μ-OH,μ-O_2 core.[3,8] The O−O bond in **1(BF$_4$)$_3$** (1.401(3) Å) is on the low end of the peroxo range (typically 1.4−1.5 Å) compared to the superoxo range (1.25−1.35 Å). Another interesting structural metric is the Co···Co distance. Considering all of the dicobalt complexes exhibiting the μ-OH,μ-O_2 core listed in Table S2, **1(BF$_4$)$_3$** exhibits the shortest distance between cobalt centers (3.18 Å). Only the Werner complex μ-OH,μ-O_2,μ-NH_2-$[(NH_3)_3Co]_2(NO_3)_3$ exhibits a shorter distance between cobalt ions [Co···Co = 2.766(4) Å].[4] This is likely due to the additional amido bridge and the higher overall oxidation state of the species (formally $Co^{III}-Co^{IV}$). The close proximity of the cobalt centers in the present case is thus likely the result of the "criss-crossed," dinucleating enN4 ligands.

Omission of excess pyridine in the reaction or any subsequent crystallization prevented isolation of the complex. We ascribe this observation to the need for pyridine in the stoichiometry of the reaction, according to eq 1:

$$2\text{enN4} + 2[Co(H_2O)_6](X)_2 + \text{py} + O_2 \rightarrow \mu\text{-OH, }\mu\text{-}O_2[\{Co(\text{enN4})\}_2]X_3 + \text{py-HX} + 11H_2O \quad (1)$$

We subsequently found a more convenient route to 1^{3+}, using $[Co(H_2O)_6](ClO_4)_2$ in place of the tetrafluoroborate salt and isolating **1(ClO$_4$)$_3$** as a precipitate directly from the reaction (37% yield); this was convenient for subsequent isotopic labeling studies (vide infra). Slow evaporation of a dilute MeCN/tol solution afforded X-ray quality crystals as **1(ClO$_4$)$_3$**·2MeCN·H_2O, confirming a nearly identical core structure to that observed in **1(BF$_4$)$_3$** (see Supporting Information, Figure S2 and Table S1). This also highlights the generality of the reaction. Solutions of both **1(BF$_4$)$_3$** and **1(ClO$_4$)$_3$** in CD_3CN exhibit ^1H NMR peaks in the diamagnetic region (Supporting Information, Figure S3 and S4), including a μ-hydroxy proton resonance observed at −0.91 ppm. In conjunction with the hydroxy proton located in the density map, this supports the overall $Co^{III}-Co^{III}$ assignment. Solutions in CD_3CN are stable in the presence of air and moisture over the course of several months.

The IR spectrum of **1(ClO$_4$)$_3$** exhibits a ligand-based ν(CN) feature at 1633 cm^{-1} (1635 cm^{-1} in **1(BF$_4$)$_3$**), which is red-shifted from the unbound ligand value of 1647 cm^{-1}. The lower energy region of **1(ClO$_4$)$_3$** exhibits notable stretches at 882, 776, and 650 cm^{-1} (887, 775, and 649 cm^{-1} for **1(BF$_4$)$_3$**).

The assignment of the ν(O−O) IR feature was verified using isotopic labeling. Metalation of enN4 with $[Co(H_2O)_6](BF_4)_2$ in MeCN in the presence of pyridine under $^{18}O_2$ atmosphere results in one red-shifted feature at 833 cm^{-1} (the $^{16}O-^{16}O$ stretch at 882 cm^{-1} is absent; see Figure 2). This confirms the ν(O−O) assignment at 882 cm^{-1} in the IR spectrum of **1(ClO$_4$)$_3$**.

We suspected that the interlinked nature of the cobalt peroxo core might stabilize reduced or oxidized species to an unusual extent. The cyclic voltammogram of **1(BF$_4$)$_3$** in MeCN (0.1 M TBAP, 100 mV/s) is shown in Figure 3. The complex exhibits a reversible feature at $E_{1/2}$ = +0.50 V vs Fc/Fc^+, as well as an irreversible feature at −1.07 V vs Fc/Fc^+. All three peak currents in the CV follow a scan rate dependence that is linear with $\sqrt{\nu}$ (inset, Figure 3; Figure S5). We hypothesized that the reversible feature was the result of clean $Co^{III}-Co^{III} \leftrightarrow Co^{III}-Co^{IV}$ transformations.

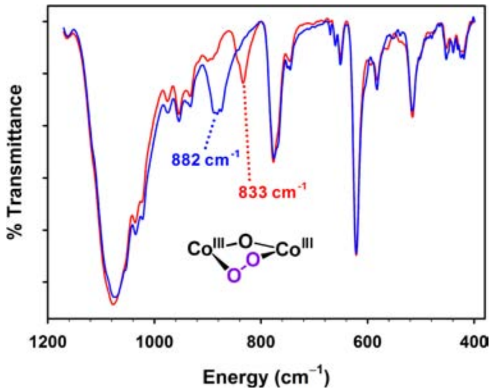

Figure 2. Infrared spectra of isotopically distinct **1(ClO$_4$)$_3$** as derived from $^{16}O_2$ (blue trace, ν_{O-O} = 882 cm^{-1}) and $^{18}O_2$ (red trace, ν_{O-O} = 833 cm^{-1}); $\Delta\nu_{expt}$ = 49 cm^{-1}, $\Delta\nu_{theory}$ = 48 cm^{-1}.

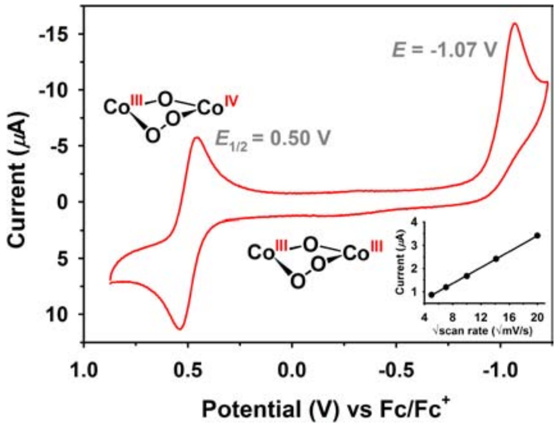

Figure 3. Cyclic voltammogram of **1(BF$_4$)$_3$** in MeCN containing 0.1 M NBu_4ClO_4 (100 mV/s). Inset: Scan rate dependence of the reversible oxidation wave at +0.54 V (see SI for scan rate dependence of other peaks).

As the oxidized species proved unisolable in our hand, we investigated its structural and electronic properties by DFT. Calculations on the species 1^{3+} at the 6-31G*/PW91 (and TZP/B3PW91) level afforded good agreement (within ~0.02 Å) between calculated and experimental bond distances (Table S2). Overall, DFT supports our assignment of a $Co^{III}-Co^{III}$ dimer bridged by a dianionic peroxide ligand. DFT calculations on the one-electron oxidized species 1^{4+} (S = 1/2) show that the spin density (Figure 4, left) is delocalized across *both* cobalt centers *and* the peroxo/superoxo ligand. By most quantitative measures (Supporting Information, Table S3), the balance of spin density tilts in favor of the peroxo (or superoxo) ligand. Some shortening (~0.07 Å) of the O−O bond is observed in the oxidized species (DFT, 1.338, 1.352 Å) versus the resting state (DFT = 1.374, 1.426 Å; exptl = 1.401(3), 1.394(3) Å). But the oxidized O−O distance in 1^{4+} is longer than the canonical superoxo bond length of ~1.25 Å.

In the absence of structural characterization, we characterized the oxidized species by EPR spectroscopy. Treatment of **1(ClO$_4$)$_3$** in MeCN with $(NH_4)_2[Ce(NO_3)_6]$ at −40 °C resulted in an immediate color change from brownish red to gray-green; this solution was not stable at higher temperatures.

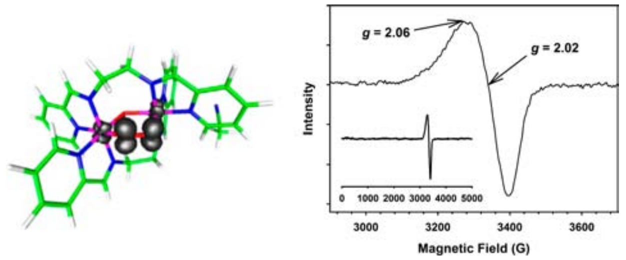

Figure 4. (Left) DFT calculated structure and spin density plot of the one-electron oxidized species 1^{4+} (6-31G*/PW91). (Right) X-band EPR spectra of an MeCN solution of $1(ClO_4)_3$ treated with 1 equiv of $(NH_4)_2[Ce(NO_3)_6]$ at −40 °C. Instrument settings: temperature, 90 K; frequency, 9.44 GHz; modulation, 100 kHz; power, 20 mW; field modulation, 5 G. Nearly identical spectra were recorded from 4 to 30 K.

EPR analysis of an aliquot from the −40 °C reaction (frozen MeCN, or MeCN/CH_2Cl_2 glass, 90 K) afforded a somewhat broad, asymmetric EPR spectrum with g values = 2.06 and 2.02 (see Figure 4, right side). No prominent hyperfine features were observed at lower temperatures (4−30 K) or upon introduction of $^{17}O_2$. The lack of prominent axial features in the spectrum (as often observed in Co^{IV} porphyrins, cobaloximes, salens)[9] is likely due to the alternate arrangement of the z axis at the cobalt center. Close inspection of the DFT calculated d_{z^2} orbital indicates that it is not oriented along an axis of bonding (see Supporting Information, Figure S6). Rather, the d_{z^2} axis trisects one face of the octahedron, eliminating its assignment as an O_h or D_{4h} type system. Some seemingly related D_3 systems like $[Fe^{III}(bpy)_3]^{3+}$ or $[Ir^{IV}(gdt)_3]^+$ reliably exhibit a primary feature at $g_\perp \approx 2.6$ (with a smaller feature, $g_\parallel = 0.3$−1.6).[10] The asymmetric N_4O_2 coordination environment in 1^{4+} appears to give rise to a minor axial component that results in an electronic environment that resembles an axially elongated D_3 system (this usually promotes high or intermediate spin systems in the Fe^{III} d^5 case). Note that the observed g values of 1^{4+} are similar to reports of cobalt-coordinated superoxo species ($g \approx 2.00$−2.08).[11] Overall, we interpret the EPR signal as emanating from an $S = 1/2$ Co^{IV} ion in a slightly axial coordination environment; this is partially consistent with the DFT calculation(s).

In summary, we synthesized a complex with a dinucleated μ-O_2,μ-OH dicobalt core using an N4 Schiff base ligand. The "criss-crossed" ligand arrangement facilitates reversible Co^{III}−Co^{III} ↔ Co^{III}−Co^{IV} processes and spectroscopic detection of the Co^{III}−Co^{IV} species. Further insight regarding the electronic structure of the oxidized species may be gained from additional EPR (Q/W-band) and/or computational (EPR prediction, simulation) studies. We are also investigating the possibility of using **1** as an electrocatalyst for peroxide oxidation/reduction, and we will report those findings in due time.

■ ASSOCIATED CONTENT

Ⓢ Supporting Information

Complete X-ray, ^1H NMR, DFT and EPR characterizations of $\mathbf{1(BF_4)_3}$ and $\mathbf{1(ClO_4)_3}$. This material is available free of charge via the Internet at http://pubs.acs.org.

■ AUTHOR INFORMATION

Corresponding Author

*E-mail: mrose@cm.utexas.edu.

Author Contributions

The manuscript was written through contributions of all authors. All authors have approved the final version of the manuscript.

Funding

This research was supported by the UT Austin College of Natural Sciences, Welch foundation (F-1822), ACS Petroleum Research Fund (PRF 53542-DN13), and the US Office of Naval Research (N00014−13−1−0530). MJR was provided funds for a DFT workstation by a Powe Junior Faculty Award.

Notes

The authors declare no competing financial interests.

■ ACKNOWLEDGMENTS

The authors acknowledge Dr Vince Lynch for collecting X-ray diffraction data and solving X-ray structures, and Minh Nguyen for EPR measurements.

■ REFERENCES

(1) Werner, A. *Liebigs Ann.* **1910**, *375*, 1.

(2) Werner, A.; Mylius, A. *Z. Anorg. Chem.* **1898**, *16*, 245.

(3) Spingler, B.; Scanavy-Grigorieff, M.; Werner, A.; Berke, H.; Lippard, S. J. *Inorg. Chem.* **2001**, *40*, 1065.

(4) (a) Ludovici, C.; Fröhlich, R.; Vogtt, K.; Mamat, B.; Lübben, M. *Eur. J. Biochem.* **2002**, *269*, 2630. (b) MacArthur, R.; Sucheta, A.; Chong, F. F. S.; Einarsdóttir, O. *Proc. Natl. Acad. Sci. U.S.A.* **1995**, *92*, 8105.

(5) (a) Wasylenko, D. J.; Palmer, R. D.; Schott, E.; Berlinguette, C. P. *Chem. Commun.* **2012**, *48*, 2107. (b) Wasylenko, D. J.; Ganesamoorthy, C.; Borau-Garcia, J.; Berlinguette, C. P. *Chem. Commun.* **2011**, *47*, 4249. (c) Askarizadeh, E.; Yaghoob, S. B.; Boghaei, D. M.; Slawin, A. M. Z.; Love, J. B. *Chem. Commun.* **2010**, *46*, 710. (d) Givaja, G.; Volpe, M.; Edwards, M. A.; Blake, A. J.; Wilson, C.; Schröder, M.; Love, J. B. *Angew. Chem., Int. Ed.* **2007**, *46*, 584.

(6) (a) McAlpin, J. G.; Surendranath, Y.; Dinca, M.; Stich, T. A.; Stoian, S. A.; Casey, W. H.; Nocera, D. G.; Britt, R. D. *J. Am. Chem. Soc.* **2010**, *132*, 6882. (b) Surendranath, Y.; Kanan, M. W.; Nocera, D. G. *J. Am. Chem. Soc.* **2010**, *132*, 16501.

(7) Calligaris, M.; Nardin, G.; Randaccio, L.; Ripamonti, A. *J. Chem. Soc. A* **1970**, 1069.

(8) (a) Zehnder, M.; Thewalt, U.; Fallab, S. *Helv. Chim. Acta* **1976**, *59*, 2290. (b) Thewalt, U.; Struckmeier, G. *Z. Anorg. Allg. Chem.* **1976**, *419*, 163. (c) Fallab, S.; Zehnder, M.; Thewalt, U. *Helv. Chim. Acta* **1980**, *63*, 1491. (d) Mäcke, H.; Zehnder, M.; Thewalt, U.; Fallab, S. *Helv. Chim. Acta* **1979**, *62*, 1804.

(9) (a) Webster, R. D.; Heath, G. A.; Bond, A. M. *J. Chem. Soc., Dalton Trans.* **2001**, 3189. (b) Harmer, J.; Doorslaer, S. B.; Gromov, I.; Bröring, M.; Jeschke, D.; Schweiger, A. *J. Phys. Chem. B* **2002**, *106*, 2801.

(10) (a) DiSimone, R. E. *J. Am. Chem. Soc.* **1973**, *95*, 6238. (b) Rohde, J.-U.; Lee, W.-T. *J. Am. Chem. Soc.* **2009**, *131*, 9162.

(11) (a) Niklas, J.; Mardis, K. L.; Rakhimov, R. R.; Mulfort, K. L.; Tiede, D. M.; Poluektov, O. G. *J. Phys. Chem. B* **2012**, *116*, 2943. (b) Green, J.; Carter, E.; Murphy, D. M. *Res. Chem. Intermed.* **2009**, *35*, 145. (c) Schrauzer, G. N.; Lee, L. P. *J. Am. Chem. Soc.* **1970**, *92*, 1551.